Adhesion Energies of Solvent Films to Pt(111) and Ni(111) Surfaces by Adsorption Calorimetry

John R. Rumptz¹ and Charles T. Campbell^{1,2*}

¹Department of Chemical Engineering, and ²Department of Chemistry

University of Washington

Seattle, Washington 98105-1700, USA

KEYWORDS. Adhesion energy, adsorption energy, solvent effects on adsorption, Pt(111), Ni(111)

Abstract

Solvent / metal adhesion energies are crucial for understanding solvent effects on adsorption energies, which are in turn central to understanding liquid-phase catalysis, electrocatalysis and many other technologies such as adsorption-based separations and chemical sensors. Differences in reactant adsorption energies in different solvents are dominated by differences in their solvent / metal adhesion energies. Here, the adhesion energies of five liquid solvents to clean Pt(111) and Ni(111) surfaces have been estimated using ultrahigh vacuum calorimetric measurements of heats of adsorption versus coverage integrated from zero coverage up to thick (bulk-like) multilayer solid films. The adhesion energies are found to vary from 0.15 to 0.60 J/m^2 , increasing in the trend CH₃OH < HCOOH < H₂O < benzene \approx phenol. This trend indicates that solvents with higher heats of adsorption per unit area in the first adsorbed layer have higher adhesion energies to a given metal surface. The adhesion energies to Ni(111) are generally larger than to Pt(111) (on average by 0.09 J/m²). This is due to the 24% higher number of metal atoms per unit area on Ni(111) than on Pt(111), and, with oxygen-containing solvents, the greater oxophilicity of Ni compared to Pt.

Keywords: solvent effects; adhesion energy; liquid / solid interface; adsorption in liquids; catalysis

^{*} charliec@uw.edu

INTRODUCTION

Catalytic and electrocatalytic reactions occurring at solid surfaces in liquid solvents are becoming increasingly important for clean energy, environmental, and chemical technologies. Detailed understanding of the kinetics of these reactions and the reasons one catalyst may be more active or more selective than another requires knowledge of the energies of the adsorbed reaction intermediates and the transition states for their surface reactions. There are accurate measurements of the energies of many adsorbed catalytic reaction intermediates on clean and well-defined metal surfaces in ultrahigh vacuum or gas phase, 1-6 and there have been a huge number of calculations of these energies using density functional theory. 4-10 In contrast, very little is known about the energies of adsorbed reaction intermediates in the presence of liquid solvents since the methods for studying surfaces in the presence of liquids are much more challenging and less developed than in the gas phase. In addition, the choice of solvent is known to have marked effects on the catalyst's activity and selectivity. 11-15 Understanding such solvent effects surely requires an understanding of how the adsorption energies of the key reaction intermediates (and transition states) depend upon the solvent, yet very little is known about this. We show below that the adhesion energy of the solvent to the solid surface (E_{adh}) is perhaps the dominant factor that determines the differences between adsorption energies in different solvents. Motivated by that observation, we report experimental measurements of adhesion energies of five different solvents to clean Pt(111) and Ni(111) surfaces extracted from our earlier calorimetric measurements of the adsorption energies of the solvent molecules on these clean metal surfaces that extended from zero coverage up to bulk-like multilayer solvent films.

The effect of solvent / solid adhesion energy on adsorption energies in solvents

As noted above, there is great motivation to leverage the vast amount we already know about the energies of adsorbates at the gas/solid or vacuum/solid interface to estimate adsorption energies on solid surfaces in the presence of liquid solvents, and to predict the effects of different solvents on adsorption energetics. Several studies have already addressed these effects. 11,12,24–33,16,34–37,17–23

We recently analyzed the differences between adsorption energies in the gas phase and in liquid solvents within a simple pairwise bond-additivity model and a standard thermodynamic-cycle approach.³⁸ That approach required that the adsorbate be a flat molecule which adsorbs parallel to the solid surface. Its accuracy was validated by comparing the heat of adsorption of phenol on Pt(111) measured in liquid water to the heat of gaseous phenol adsorption on Pt(111) measured in ultrahigh vacuum.^{38–40}

We reproduce that model in Fig. 1, but present it here in a more general form than we suggested when first presenting it, i.e., by replacing water with the general solvent "S" and the metal surface (Pt(111)) with the general material surface "M". (We refer to M as a metal below, but the analysis applies to any solid material.) The adsorbing reactant "R" is any flat molecule like phenol. We imagine here a vertical column of solvent with a cross sectional area equal to the area required for one adsorbed molecule of R (σ_R). Since the molecule R is flat (one atom

thick), edge effects on energies were assumed to be negligible, but we argued that this model should also be applicable to thicker molecules when reasonably flat.³⁸

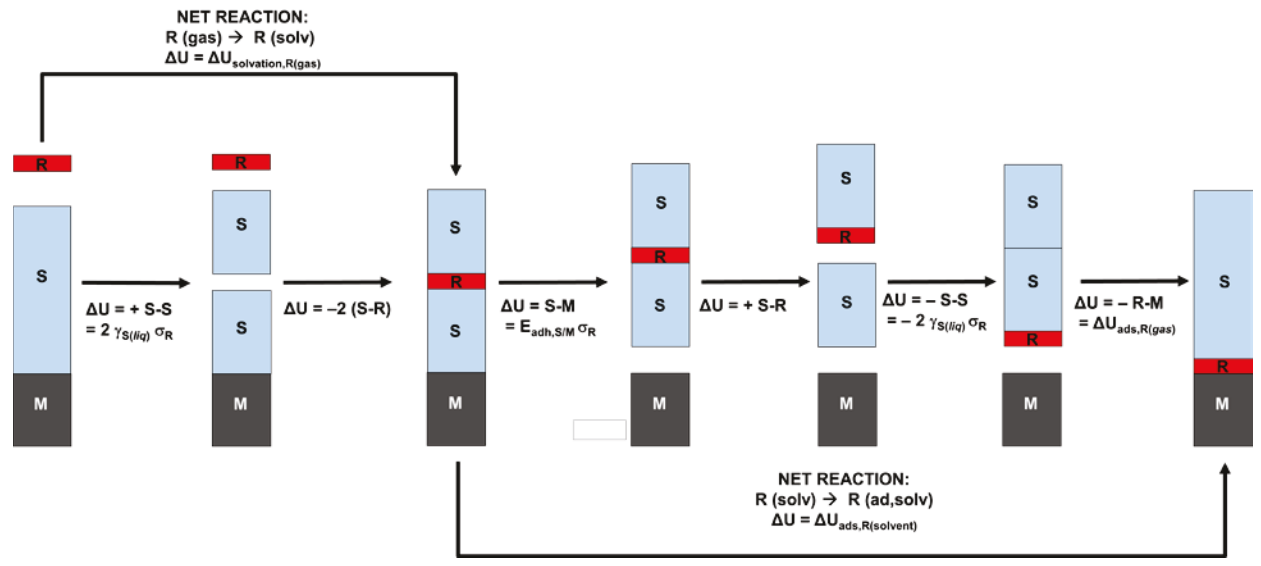


Figure 1. Thermodynamic cycle using pairwise bond additivity to relate the energy of adsorption of a flat reactant molecule (R) onto a clean metal surface (M) in gas phase (– R-M) with that measured in a solvent (S). Here we show each step's change in internal energy (ΔU) at the temperature of interest. The surface energy ($\gamma_{S(liq)}$) and adhesion energy (E_{adh}) are energies per unit area, so these are multiplied by the area per adsorbed R molecule (σ_R).

In this bond additivity model the first two steps, when combined, are just the solvation of R(gas) in liquid S to make solvated R, or R(solv). The energy for these two combined steps (shown as the arrow across the top) is $\Delta U_{solvation,R(gas)}$. Its value is often able to be determined using the reported experimental temperature dependence of Henry's Law constant (or the solubility constant) for R(gas) in S, as we did for phenol in water (giving $\Delta U_{solvation,phenol(gas)} = -47.5 \text{ kJ/mol}).^{38,41}$ In the first step, the solvent-solvent bonding in the area of one R molecule must be broken to make two vacuum / solvent interfaces. The energy cost for this is called S-S, for the solvent-solvent bond energy. The value of S-S is by definition twice the surface energy of the liquid solvent at its gas or vacuum interface ($\gamma_{S(liq)}$) multiplied by the surface area occupied by one R molecule, σ_R . One can estimate this energy change using the reported experimental surface free energy of liquid solvent, since it is generally dominated by the energy cost to break the strong solvent-solvent bonding with only small contributions from entropy. The two solvent surfaces are then bonded to both sides of a gaseous R molecule, which is downhill in energy by twice the solvent-R bond energy over the area of one R, or 2(S-R). The net reaction depicted in the top arrow then has energy:

$$\Delta U_{\text{solvation},R(\text{gas})} = S-S - 2(S-R) = 2[(\gamma_{S(\text{lig})} \cdot \sigma_R) - S-R]. \tag{1}$$

One can set this equal to the experimental $\Delta U_{solvation,R(gas)}$ for steps 1 plus 2 combined (if known) and solve for S-R to get:

$$S-R = -\Delta U_{solvation,R(gas)}/2 + (\gamma_{S(liq)} \cdot \sigma_R). \tag{2}$$

When applied to phenol in water, this equation gave S-R = 50.1 kJ per mole of phenol surface area.³⁸

The next step is to separate the solvent from the metal, which is uphill in energy by S-M, equal by definition to the solvent/metal adhesion energy per unit area times the area required for the adsorbed reactant, $E_{adh,S/M} \cdot \sigma_R$. Next, the solvent column below the R is separated from the R, which has energy cost of S-R, as given by Eq. (2). The lower solvent column is next attached to the upper solvent column, which is downhill in energy by the S-S bond energy, i.e., $\Delta U = -S - S = -2 \ (\gamma_{S(liq)} \cdot \sigma_R)$. Finally, the bottom of the solvent column (which is now terminated in molecule R) is attached to the metal surface. This last step is downhill by the molecule-metal surface bond energy, $\Delta U = R$ -M, which in this simple bond-additivity model is assumed to be the same as the adsorption energy in the gas phase, $\Delta U_{ads,R(gas)}$. As shown by the bottom arrow, these last four steps combine to make the net reaction (from R in solvent plus M in solvent to R adsorbed on M in solvent), or the solvent-phase adsorption of R. Therefore, the energy for this net solvent-phase adsorption reaction, $\Delta U_{ads,R(solvent)}$, is just the sum of energies for each of these four steps:

$$\Delta U_{ads,R(solvent)} = S-M + S-R - S-S - R-M ,$$

$$\Delta U_{ads,R(solvent)} = E_{adh,S/M} \cdot \sigma_R + S-R - 2 (\gamma_{S(lig)} \cdot \sigma_R) + \Delta U_{ads,R(gas)}.$$
 (3)

Substituting for S-R from Eq. (2) into Eq. (3) above gives:

or

$$\begin{split} \Delta U_{ads,R(solvent)} &= E_{adh,S/M} \cdot \sigma_R - \Delta U_{solvation,R(gas)}/2 + (\gamma_{S(liq)} \cdot \sigma_R) - 2 \; (\gamma_{S(liq)} \cdot \sigma_R) + \Delta U_{ads,R(gas)} \\ &= E_{adh,S/M} \cdot \sigma_R - \Delta U_{solvation,R(gas)}/2 - (\gamma_{S(liq)} \cdot \sigma_R) + \Delta U_{ads,R(gas)} \;\;, \\ or \\ \Delta U_{ads,R(solvent)} &= \Delta U_{ads,R(gas)} + E_{adh,S/M} \cdot \sigma_R - \Delta U_{solvation,R(gas)}/2 \;\; - \; \gamma_{S(liq)} \cdot \sigma_R \;\;. \end{split}$$

Note that the last two terms in this equation are often known from the bulk behavior of the liquid solvent (and its solvation of R), provided the area covered by adsorbed R can be estimated. Thus, Eq. (4) provides a simple way to estimate the adsorption energy in a solvent from its adsorption energy in vacuum, provided the adhesion energy of the solvent to the solid surface is known. Alternatively, Eq. (4) provides a potentially useful way to estimate this adhesion energy if any molecule's adsorption energy has been measured in both vacuum and this solvent.

We emphasize that *this is a very simple model*. Most importantly, it would have large error if there were a large amount of charge transfer between the adsorbate and the metal. Thus, it is designed for neutral adsorbates, not adsorbed anions or cations. While this is a severe limitation, the fact is that the computational catalysis community is still struggling with how to accurately include solvent effects in even the simplest adsorption systems. Thus, the simplicity of experimental systems it can treat and its simple elementary-step breakdown of the process in Fig. 1 offers important advantages in that it can provide simple experimental benchmarks for testing computational models for solvent effects.

Equation (4) shows that the solvent-phase adsorption energy is markedly less exothermic than the gas phase $\Delta U_{ads,R(gas)}$ due to the adhesion energy of the solvent to the metal and the exothermicity of solvation of the gas. We applied Equations (3) and (4) to aqueous-phase phenol adsorption on Pt(111) and found that the dominant difference between $\Delta U_{ads,R(solvent)}$ and $\Delta U_{ads,R(gas)}$ was the adhesion energy term, $E_{adh,S/M} \cdot \sigma_R$, which is ~116 kJ per mol phenol for that case. The two terms $-\Delta U_{solvation,R(gas)}/2$ and $-\gamma_{S(liq)} \cdot \sigma_R$ were both much smaller in magnitude (~26 kJ per mol phenol) and they had opposite signs, so they nearly cancelled. This observation suggests that differences in $E_{adh,S/M}$ between different solvents may often be the largest contribution that determines the differences in energy between adsorption of the same molecule on the same surface in different solvents. This important effect of the solvent/metal adhesion energy on adsorption energies provides strong motivation for making experimental estimates of solvent/metal adhesion energies for other systems. We report below nine new experimental estimates of solvent / metal adhesion energies which show that E_{adh} varies strongly with the solvent and is generally larger to Ni(111) than Pt(111).

When we introduced the concepts in Fig. 1 and Eq. (4),³⁸ we also presented a similar thermodynamic cycle ("Scheme 4") that used the adsorption energy of the solvent in the first layer instead of the adhesion energy. That cycle made the assumption that the solvent-solvent bond energy between the 1st and 2nd layers of solvent is the same as in the bulk of the solvent. That assumption is only approximately correct. The raw heat versus coverage data cited in Table 1 shows that the heat of adsorption in the 2nd layer is generally ~5 to 20% larger than in the 3rd and thicker layers. So using Eq. (4) and adhesion energies is more accurate than using only first-layer adsorption energies within that Scheme 4. The difference is 12.4 kJ/mol for phenol adsorption on Pt(111) in water.³⁸ Perhaps more importantly, using Scheme 4 requires knowing the exact coverage where the first layer completes and the 2nd layer starts. This is not always possible to accurately determine from the experiments. The use of adhesion energies and Eq. (4) completely avoids the need to do that.

Solvent / metal adhesion energies

To our knowledge, there is presently no known way to directly measure the adhesion energy of any liquid solvent to any clean surface. However, we have repeatedly measured solid/solid adhesion energies sincege 1997 using a method we developed based on calorimetric

heats of vapor adsorption onto clean solid surfaces in ultrahigh vacuum (UHV) whose accuracy has been validated. This method involves integrating the measured heat of adsorption from zero coverage up to a high coverage where the vapor has grown a thick (bulk-like) solid multilayer. Until our recent report of E_{adh} for water(solid) / Pt(111) interface, we had only used this approach to measure E_{adh} for solid *metal* films on clean oxide and metal surfaces. We will use that same approach here to estimate the adhesion energies of bulk-like films of five different *solvents* (water, methanol, formic acid, benzene, phenol) to clean Pt(111) and Ni(111) surfaces.

We will use the same equation as derived in ref. 42 for measuring adhesion energies of solid metal films to clean single-crystal surfaces, only now applying it to the adhesion energy of solvents onto clean Pt(111) or Ni(111) surfaces. Figure 2 shows the thermodynamic cycle used to derive the needed equation, adapted from ref. 42 to the different species involved here, with S referring to the solvent species. The calorimetric measurement is depicted as the arrow that goes from the top state (n molecules of gaseous S plus a clean solid surface of material M with area A in UHV) down to the state at the bottom right, a multilayer slab of condensed liquid solvent S on the solid surface. The enthalpy change for this step is just the sum of the enthalpies of adsorption of all n molecules of S, equal to the negative of the heat of adsorption integrated over the coverage range from 0 to n/A, or $-Q_{adsorption}$.

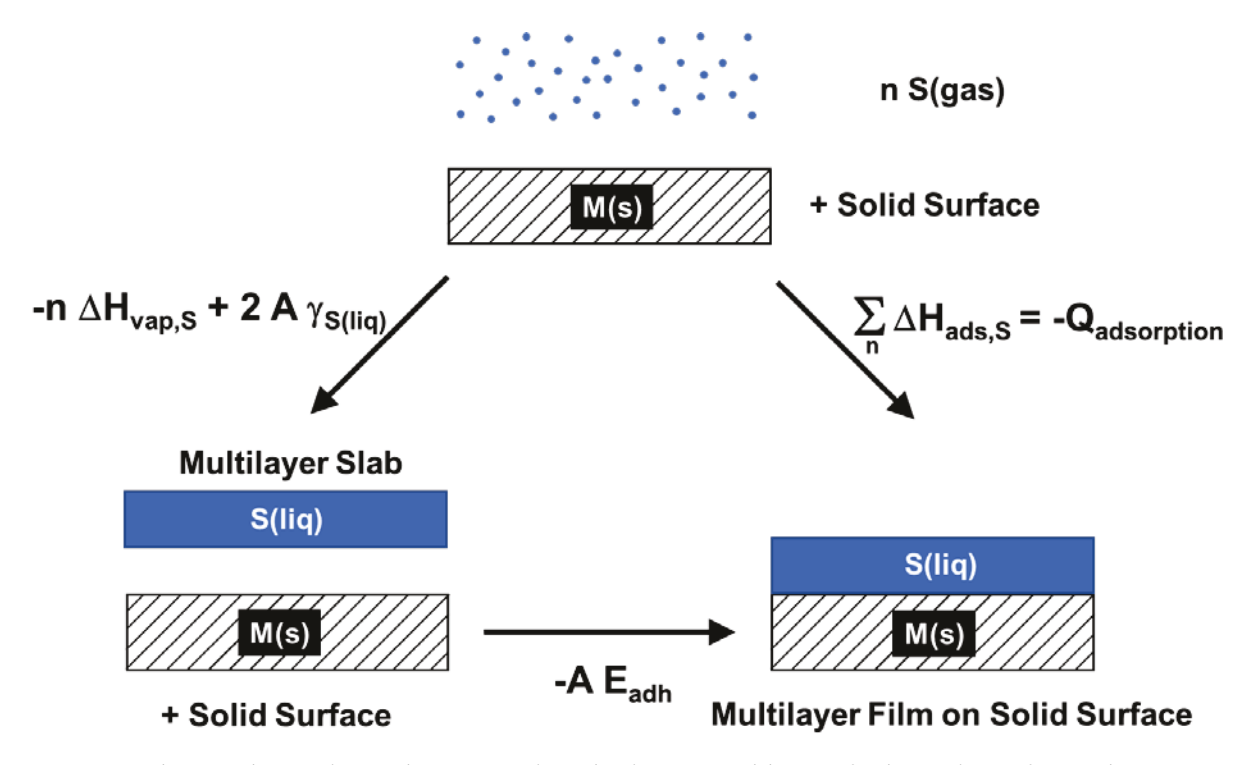


Figure 2. Thermodynamic cycle connecting the integrated heat of adsorption of gas phase solvent molecules (S) to its adhesion energy (E_{adh}) for a thick multilayer film of S(liq) on a surface of some solid material (M) covering some surface area (A).

The same net reaction can be realized by first taking the arrow down to the left to condense the n solvent molecules into a free-standing multilayer slab of pure S liquid, S(liq), and then taking the arrow from the bottom left to right attaching the liquid slab of S to the solid surface. The first step has an enthalpy change equal to negative n times the bulk heat of vaporization of pure S $(-n \cdot \Delta H_{vap,S})$, plus two times the surface energy of the pure liquid S times the area $(2 \text{ A} \cdot \gamma_{S(liq)})$. The energy for the second step is, by definition, just equal to the area times the adhesion energy $(-A \cdot E_{adh,S(liq)/M(s)})$. The enthalpy change for the second step is equal to its energy change since there is no significant change in volume. The sum of enthalpy changes for all three steps in the cycle must sum to zero, so that:

$$-A \cdot E_{adh,S(liq)/M(s)} = +(n \cdot \Delta H_{vap,S} - 2A \cdot \gamma_{S(liq)}) - Q_{adsorption}. \tag{5}$$

This can be rearranged to give:

$$E_{adh,S(liq)/M(s)} = [Q_{adsorption} - n \cdot \Delta H_{vap,S}]/A + 2 \cdot \gamma_{S(liq)}.$$
 (6)

Since the heats of vaporization and surface energies are known for many liquid solvents at room temperature, the integrated heat of adsorption of S(gas) per unit area ($Q_{adsorption}/A$) provides all that is needed to apply this equation to estimate the solvent/metal adhesion energy.

Unfortunately, $Q_{adsorption}$ can only be measured at lower temperatures, where the solvents grow as solid films rather than liquid films. For that reason, we make the assumption that the first term here, $[Q_{adsorption} - n \cdot \Delta H_{vap,S}]/A$ at room temperature, is approximately equal to the analogous quantity which we can measure at low temperatures when S is a solid: $[Q_{adsorption} - n \cdot \Delta H_{sub,S}]/A$, where $\Delta H_{sub,S}$ is the bulk heat of sublimation of pure S. The assumption that this equals $[Q_{adsorption} - n \cdot \Delta H_{vap,S}]/A$ at room temperature is based on our expectation that the zero-Kelvin chemical bond energies dominate these energies at all temperatures. It is equivalent to assuming that the first two layers and multilayers have the same difference in heat capacities at all temperatures. This is similar to the assumption of zero difference in heat capacities made in deriving both the famous Clausius-Clapeyron and van't Hoff Equations, 44 but it is less accurate since the heat of fusion is involved here in the multilayers and possibly also in the near-surface layers. Since the heat of fusion is small compared to the heat of sublimation, this is expected to be a small error.

Figure 3 shows an example of such a heat of adsorption versus coverage measurement, for the case of formic acid adsorption on Ni(111) at 120 K from ref. ⁴⁵. All such data were measured in ultrahigh vacuum by single crystal adsorption calorimetry (SCAC). As seen, the heat of adsorption is high until the first layer is saturated, and it drops down to near (but still above) the heat of sublimation of the pure, thick multilayer ($\Delta H_{sub,S}$) in the second layer, but closely approaches this high-coverage asymptotic limit of $\Delta H_{sub,S}$ by the third layer. This decrease is typical of all the systems analyzed here. The quantity $[Q_{adsorption} - n \cdot \Delta H_{sub,S}]/A$ is just

the shaded area shown. As was derived above, this quantity added to twice the surface free energy of the solvent yields the adhesion energy between the solvent and the metal surface.

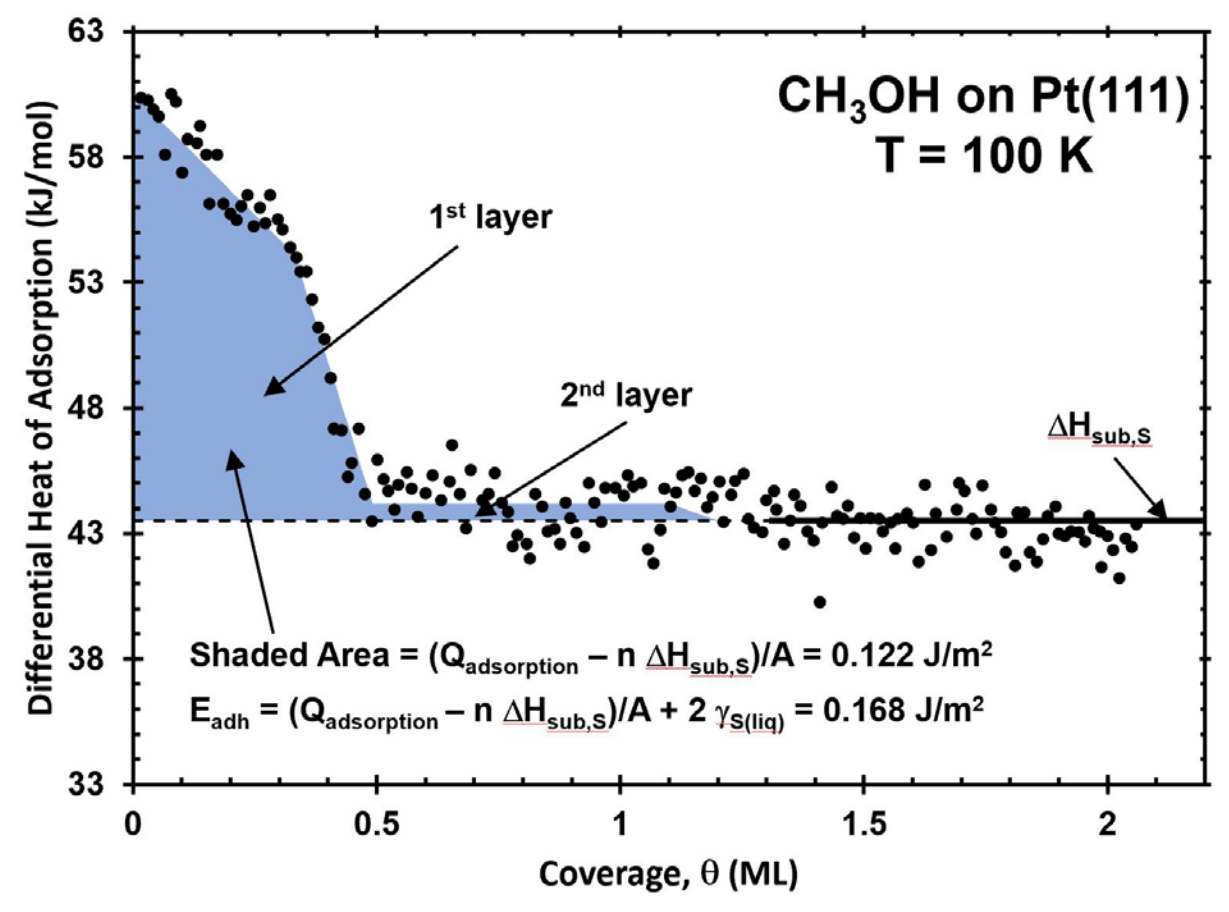


Figure 3. Heat of adsorption of methanol gas versus coverage on Pt(111) at 100 K measured by SCAC, from ref. ⁴⁶. The coverage axis here is in absolute units of "monolayers" or ML, defined as the number of methanol molecules per Pt(111) surface atom where 1 ML corresponds to the surface atom density of Pt(111) (1.51 x10¹⁵ molecules / cm²). The first layer saturates at a coverage of ½ ML. The shaded area is the quantity $[Q_{adsorption} - n \cdot \Delta H_{sub,S}]/A$ used to estimate $[Q_{adsorption} - n \cdot \Delta H_{vap,S}]/A$ when applying Eq. (6) to estimate the adhesion energy.

The adhesion energies for thin multilayer films of solvent molecules on Pt(111) and Ni(111) determined from SCAC data like those in Fig. 3 using Eq. (6) are summarized in Table 1. Also listed there are the experimental surface energies (γ_i) and sublimation energies used in Eq. (6) and their sources.

Table 1: Adhesion Energies of Solvent Films to Single Crystal Metal Surfaces

Solvent	Metal	T (K)	$\gamma_{S(liq)}$ (J/m ²)	ΔH _{sub,S} (kJ/mol)	E _{adh} (J/m ²)	(Q _{ads} - $n\Delta H_{sub,S}$)/A (J/m ²)
D_2O	Pt(111)	88	0.0730	48.1	0.273	0.127
	Pt(111)	120	0.0730	47.2	0.230	0.084
	Ni(111)	100	0.0730	46.9	0.345	0.199
CH₃OH	Pt(111)	100	0.0230	43.8	0.168	0.122
	Ni(111)	100	0.0230	44.0	0.217	0.171
НСООН	Pt(111)	100	0.0377	52.8	0.162	0.086
	Ni(111)	120	0.0377	49.9	0.279	0.204
C_6H_6	Pt(111)	90	0.0288	73.2 44.2	0.447	0.389
	Ni(111)	90	0.0288	72.2 44.5	0.600	0.542
$C_6^{}H_5^{}OH$	Pt(111)	90	0.0400	4 4.2 73.2	0.463	0.383
	Ni(111)	150	0.0400	44.5 72.2	0.501	0.421

Surface energies of pure liquids of molecular species $(\gamma_{S(liq)})$ are from refs. ^{47–49}. Their heats of sublimation (ΔH_{sub}) at the measurement temperature are taken to be equal to the high-coverage limits for their heats of adsorption from the SCAC measurements used to get $Q_{adsorption}/A$, i.e., from refs. ^{39,45,46,50–54}, as was proven in those papers to be true to within the accuracy of the absolute calibration of the calorimeter heat signal (3%). Adhesion energies (E_{adh}) were determined by using the above values in Eq. (6), assuming that $[Q_{adsorption} - n \cdot \Delta H_{vap,S}]/A$ at room temperature equals $(Q_{adsorption} - n \cdot \Delta H_{sub,S})/A$ here.

Figure 4 summarizes the adhesion energies from Table 1. As seen, the adhesion energies to Pt(111) increase in the sequence $CH_3OH < HCOOH < H2O <$ benzene \approx phenol, and the values to Ni(111) follow the same sequence except that they are generally larger than to Pt(111) (on average by 0.09 J/m^2 or 37%) and phenol is instead lower than benzene. Note that these values reflect the internal energy contributions only. They do not include any entropic contributions.

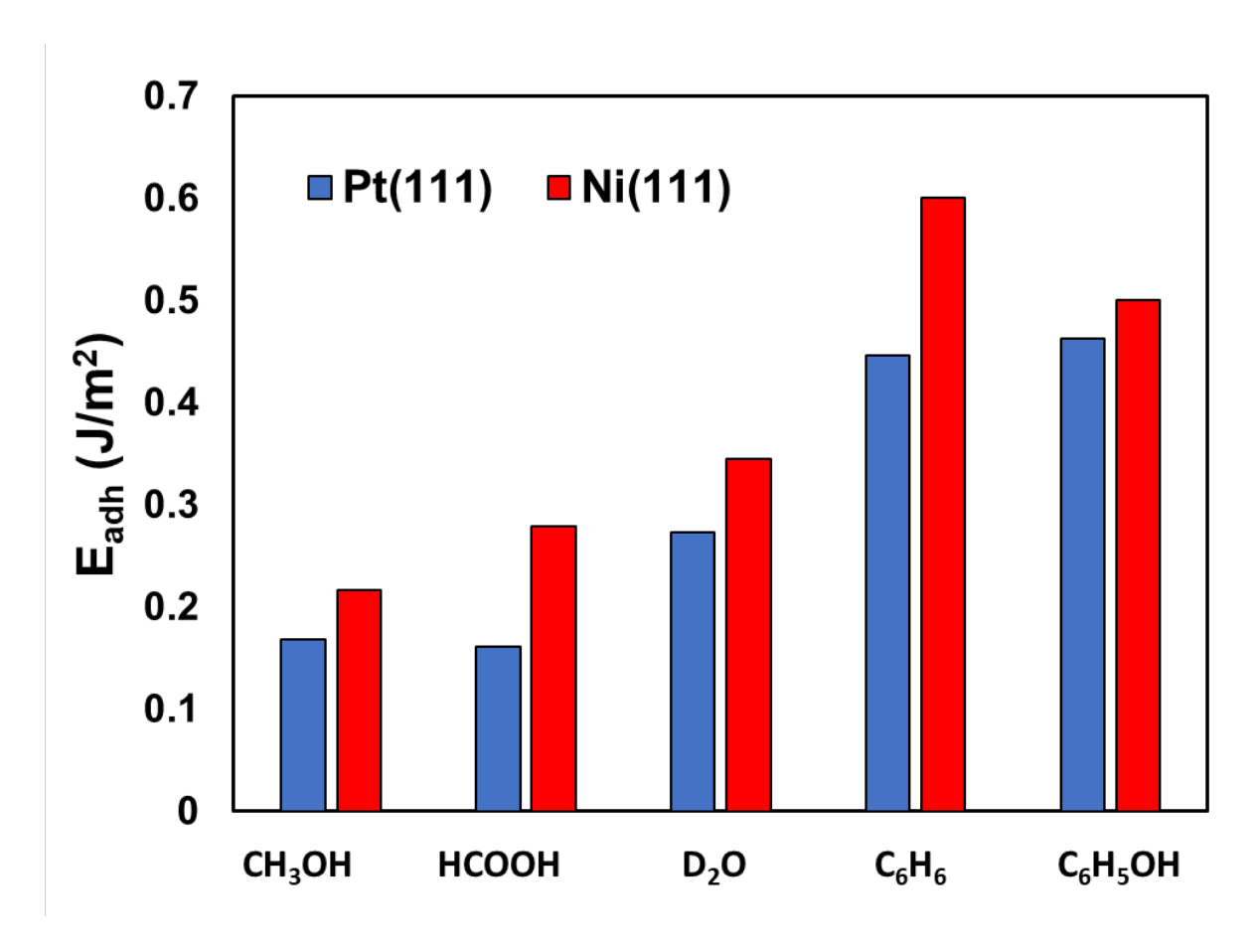


Figure 4: Adhesion energies for each liquid solvent on clean Pt(111) and Ni(111) surfaces determined using Eq. (6) together with low-temperature calorimetric heats of adsorption. See Table 1 for temperatures used.

The larger adhesion energy of the oxygen-containing solvents on Ni(111) in comparison to Pt(111) is likely a result of the larger oxophilicity of Ni compared with Pt. Previous work by our group has shown that the -OR bond energies to Ni(111) are ~70 kJ/mol larger than their bond energies to Pt(111),⁵⁵ reflecting the well-known greater oxophilicity of Ni. This leads to stronger adhesion of the oxygen-containing solvents (i.e., all except benzene) to Ni(111) than Pt(111). For benzene, the heats of adsorption versus coverage (per surface metal atom) is almost identical on Ni(111) and Pt(111).⁵¹ However, the number of metal atoms per unit area is 24% larger on Ni(111) than on Pt(111), so this leads to a stronger adhesion energy per unit area for benzene on Ni(111) than Pt(111).

The trend in Fig. 4 of adhesion energy with different solvent molecules is quite similar on both Pt(111) and Ni(111). As one moves to the right in Fig. 4, the observed increase is E_{adh} is dominated by the increase in the $[Q_{adsorption} - n \cdot \Delta H_{sub,S}]/A$ term in Table 1. Close inspection of the heats of adsorption versus coverage reveals that this term is dominated by the heat of

adsorption in the first layer of adsorbed molecules that are in direct contact with the metal surface. Thus, one can approximately state that the solvents with higher heats of adsorption per unit area in the first adsorbed layer have higher adhesion energies. A variety of physical effects contribute to the heat of adsorption per unit area for any given molecularly-adsorbed solvent molecule, so any further discussion of this trend in Fig. 4 would require an in-depth analysis with the aid of quantum mechanics calculations.

We have recently used a very similar approach to estimate the adhesion energy of water to Pt(111) using the same calorimetric values for $[Q_{adsorption} - n \cdot \Delta H_{sub,S}]/A$ as listed in Table 1.³⁸ However, in that case we estimated E_{adh} of solid water to Pt(111) rather than liquid water, so that the term $2 \cdot \gamma_{S(liq)}$ in Eq. (6) here was replaced with that for solid water, $2 \cdot \gamma_{S(solid)}$ (which for solid water is 0.109 J/m²).⁵⁶ This solid-water surface energy is 0.036 J/m² larger than that for liquid water, so it gave $E_{adh} = 0.32 \text{ J/m}^2$, averaged over the two temperatures of the calorimetry experiments (0.345 and 0.302 J/m² at 88 and 120 K, respectively). The liquid E_{adh} value in Table 1 (also averaged for these two temperatures) is 0.07 J/m² (or 22%) smaller. Since we could not find $\gamma_{S(solid)}$ values from the literature for the *solid* surfaces of other solvent molecules, we cannot make this comparison for them. However, since the other solvents have liquid surface energies that are ~40 to 70% smaller than for water, we expect a smaller absolute difference between estimated solid versus liquid adhesion energies than this 0.07 J/m² difference seen for water. This would not have much of an effect on the trends in E_{adh} plotted in Fig. 4, which would still hold if using these solid solvent values instead. For the water on Ni(111) system, using the surface energy for ice stated above leads to a calculated adhesion energy of 0.417 J/m² at 100 K which is also 0.075 J/m² (or 22%) larger than the liquid value of 0.342 J/m² listed in Table 1.

As with the examples above for water, in general, the surface energy of the solid will be larger than that of the liquid as shown in the well-known relationship:⁵⁷

$$\gamma$$
Solid $\geq \gamma$ Liquid + γ Solid/Liquid . (7)

It follows that the adhesion energies reported here will be systematically smaller than the true value obtained from using the solid surface energy. Results investigating the surface energy of pure metals suggest a constant ratio of the solid to liquid surface energy with a value of $\gamma_{\text{Solid}}/\gamma_{\text{Liquid}} \approx 1.18.^{57}$ Using this ratio to estimate the solid surface energies of the solvents in Table 1 leads to the conclusion that the 18% increase in the surface energy (from liquid to solid) leads to an average increase of only ~6% in the calculated adhesion energy due to the dominance of the term $[Q_{adsorption} - n \cdot \Delta H_{sub,S}]/A$ in the adhesion energy calculation.

The adhesion energy between two condensed phases or materials is defined as the energy per unit area required to separate them to form two distinct surfaces. For a solvent S and a material M, this is reflected in Eq. 8.

$$E_{adh} = \gamma_M + \gamma_S - \gamma_{S/M}. \tag{8}$$

Based on the values reported in Table 1 for adhesion energies and solvent surface energies, and using the reported surface energies of pure metals ($\gamma_{Pt(111)} = 2.49 \text{ J/m}^2$ and $\gamma_{Ni(111)} = 2.38 \text{ J/m}^2$), 57,58 it is straightforward to use this equation to calculate the surface energy of the solvent/metal interface. This interfacial energy often appears in equations relating to the wetting of a material substrate, 59,60 so its calculation from the above data may be useful to some readers.

CONCLUSIONS

Using cryogenic calorimetric measurements of the heats of adsorption of solvent molecules on clean Pt(111) and Ni(111) surfaces as a function of coverage up to high coverages where the molecules grow thick (bulk-like) solid films, we have extracted the adhesion energies per unit area of five liquid solvents (methanol, formic acid, water, benzene and phenol) on Pt(111) and Ni(111). The results are summarized in Figure 4. To estimate these adhesion energies, we assumed that the measured heat of adsorption in the first few layers is the same amount above the multilayer heat on these cold surfaces (i.e., at ~100 K) as it would be if measured near room temperature where the solvent is a liquid. This leads to some error, estimated to be small compared to the differences between solvents in Figure 4. These adhesion energies can be used in thermodynamic cycles, like the bond-additivity model in Figure 1, to help clarify solvent effects on adsorption energies and the rates of liquid phase catalytic and electrocatalytic reactions.

AUTHOR INFORMATION

Corresponding Author

* Charles T. Campbell: charliec@uw.edu

Author Contributions

This model was developed and this manuscript was written through contributions of all authors. All authors have given approval to the final version of the manuscript.

Notes

The authors declare no competing financial interest.

ACKNOWLEDGEMENTS

The authors gratefully acknowledge Professors Nirala Singh, Johannes A. Lercher and Líney Árnadóttir for very helpful discussions. They acknowledge financial support by the DOE-OBES Chemical Sciences Division under Grant #DE-FG02-96ER14630 and the National Science Foundation under Grant #CHE-1665077.

REFERENCES

- (1) Campbell, C. T. Energies of Adsorbed Catalytic Intermediates on Transition Metal Surfaces: Calorimetric Measurements and Benchmarks for Theory. *Acc. Chem. Res.* **2019**, *52*, 984–993.
- (2) Brown, W. A.; Kose, R.; King, D. A. Femtomole Adsorption Calorimetry on Single-Crystal Surfaces. *Chem. Rev.* **1998**, *98*, 797–832.
- (3) Silbaugh, T. L.; Campbell, C. T. Energies of Formation Reactions Measured for Adsorbates on Late Transition Metal Surfaces. *Journal of Physical Chemistry C*. 2016, pp 25161–25172.
- (4) Wellendorff, J.; Silbaugh, T. L.; Garcia-Pintos, D.; Nørskov, J. K.; Bligaard, T.; Studt, F.; Campbell, C. T. A Benchmark Database for Adsorption Bond Energies to Transition Metal Surfaces and Comparison to Selected DFT Functionals. *Surf. Sci.* **2015**, *640*, 36–44.
- (5) Dementyev, P.; Dostert, K. H.; Ivars-Barcelõ, F.; O'Brien, C. P.; Mirabella, F.; Schauermann, S.; Li, X.; Paier, J.; Sauer, J.; Freund, H. J. Water Interaction with Iron Oxides. *Angew. Chemie Int. Ed.* **2015**, *54*, 13942–13946.
- (6) Montemore, M. M.; Van Spronsen, M. A.; Madix, R. J.; Friend, C. M. O2 Activation by Metal Surfaces: Implications for Bonding and Reactivity on Heterogeneous Catalysts. *Chem. Rev.* **2018**, *118*, 2816–2862.
- (7) Norskov, J. K.; Abild-Pedersen, F.; Studt, F.; Bligaard, T. Density Functional Theory in Surface Chemistry and Catalysis. *Proc. Natl. Acad. Sci.* **2011**, *108*, 937–943.
- (8) Ruiz, V. G.; Liu, W.; Zojer, E.; Scheffler, M.; Tkatchenko, A. Density-Functional Theory with Screened van Der Waals Interactions for the Modeling of Hybrid Inorganic-Organic Systems. *Phys. Rev. Lett.* **2012**, *108*.
- (9) Gautier, S.; Steinmann, S. N.; Michel, C.; Fleurat-Lessard, P.; Sautet, P. Molecular Adsorption at Pt(111). How Accurate Are DFT Functionals? *Phys. Chem. Chem. Phys.* **2015**, *17*, 28921–28930.
- (10) Mavrikakis, M. Computational Methods: A Search Engine for Catalysts. *Nat. Mater.* **2006**, *5*, 847–848.
- (11) Walker, T. W.; Chew, A. K.; Li, H.; Demir, B.; Zhang, Z. C.; Huber, G. W.; Van Lehn, R. C.; Dumesic, J. A. Universal Kinetic Solvent Effects in Acid-Catalyzed Reactions of Biomass-Derived Oxygenates. *Energy Environ. Sci.* **2018**, *11*, 617–628.
- (12) Mellmer, M. A.; Sener, C.; Gallo, J. M. R.; Luterbacher, J. S.; Alonso, D. M.; Dumesic, J. A. Solvent Effects in Acid-Catalyzed Biomass Conversion Reactions. *Angew. Chemie Int. Ed.* 2014, 53, 11872–11875.
- (13) Mellmer, M. A.; Sanpitakseree, C.; Demir, B.; Bai, P.; Ma, K.; Neurock, M.; Dumesic, J. A. Solvent-Enabled Control of Reactivity for Liquid-Phase Reactions of Biomass-Derived Compounds. *Nat. Catal.* **2018**, *1*, 199–207.
- (14) Qi, L.; Alamillo, R.; Elliott, W. A.; Andersen, A.; Hoyt, D. W.; Walter, E. D.; Han, K. S.; Washton, N. M.; Rioux, R. M.; Dumesic, J. A.; Scott, S. L. Operando Solid-State NMR Observation of Solvent-Mediated Adsorption-Reaction of Carbohydrates in Zeolites. *ACS Catal.* **2017**, *7*, 3489–3500.
- (15) He, J.; Liu, M.; Huang, K.; Walker, T. W.; Maravelias, C. T.; Dumesic, J. A.; Huber, G. W. Production of Levoglucosenone and 5-Hydroxymethylfurfural from Cellulose in Polar

- Aprotic Solvent-Water Mixtures. Green Chem. 2017, 19, 3642–3653.
- (16) Bockris, J. O. M.; Jeng, K. T. In-Situ Studies of Adsorption of Organic Compounds on Platinum Electrodes. *J. Electroanal. Chem.* **1992**, *330*, 541–581.
- (17) Kristoffersen, H. H.; Shea, J.-E.; Metiu, H. Catechol and HCl Adsorption on TiO2(110) in Vacuum and at the Water–TiO2 Interface. *J. Phys. Chem. Lett.* **2015**, *6*, 2277–2281.
- (18) Song, W.; Martsinovich, N.; Heckl, W. M.; Lackinger, M. Born-Haber Cycle for Monolayer Self-Assembly at the Liquid-Solid Interface: Assessing the Enthalpic Driving Force. *J. Am. Chem. Soc.* **2013**, *135*, 14854–14862.
- (19) Song, W.; Martsinovich, N.; Heckl, W. M.; Lackinger, M. Thermodynamics of Halogen Bonded Monolayer Self-Assembly at the Liquid-Solid Interface. *Chem. Commun.* **2014**, *50*, 13465–13468.
- (20) Song, W.; Martsinovich, N.; Heckl, W. M.; Lackinger, M. Thermodynamics of 4,4'-Stilbenedicarboxylic Acid Monolayer Self-Assembly at the Nonanoic Acid-Graphite Interface. *Phys. Chem. Chem. Phys.* **2014**, *16*, 13239–13247.
- (21) Yoon, Y.; Rousseau, R.; Weber, R. S.; Mei, D.; Lercher, J. A. First-Principles Study of Phenol Hydrogenation on Pt and Ni Catalysts in Aqueous Phase. *J. Am. Chem. Soc.* **2014**, *136*, 10287–10298.
- (22) Singh, N.; Nguyen, M. T.; Cantu, D. C.; Mehdi, B. L.; Browning, N. D.; Fulton, J. L.; Zheng, J.; Balasubramanian, M.; Gutiérrez, O. Y.; Glezakou, V. A.; Rousseau, R.; Govind, N.; Camaioni, D. M.; Campbell, C. T.; Lercher, J. A. Carbon-Supported Pt during Aqueous Phenol Hydrogenation with and without Applied Electrical Potential: X-Ray Absorption and Theoretical Studies of Structure and Adsorbates. *J. Catal.* **2018**, *368*, 8–19.
- (23) Singh, N.; Lee, M. S.; Akhade, S. A.; Cheng, G.; Camaioni, D. M.; Gutiérrez, O. Y.; Glezakou, V. A.; Rousseau, R.; Lercher, J. A.; Campbell, C. T. Impact of PH on Aqueous-Phase Phenol Hydrogenation Catalyzed by Carbon-Supported Pt and Rh. *ACS Catal.* **2019**, *9*, 1120–1128.
- (24) Gray, C. M.; Saravanan, K.; Wang, G.; Keith, J. A. Quantifying Solvation Energies at Solid/Liquid Interfaces Using Continuum Solvation Methods. *Mol. Simul.* **2017**, *43*, 420–427.
- (25) Montemore, M. M.; Andreussi, O.; Medlin, J. W. Hydrocarbon Adsorption in an Aqueous Environment: A Computational Study of Alkyls on Cu(111). *J. Chem. Phys.* **2016**, *145*.
- (26) She, Z. W.; Kibsgaard, J.; Dickens, C. F.; Chorkendorff, I.; Nørskov, J. K.; Jaramillo, T. F. Combining Theory and Experiment in Electrocatalysis: Insights into Materials Design. *Science*. American Association for the Advancement of Science January 13, 2017.
- (27) Calle-Vallejo, F.; De Morais, R. F.; Illas, F.; Loffreda, D.; Sautet, P. Affordable Estimation of Solvation Contributions to the Adsorption Energies of Oxygenates on Metal Nanoparticles. *J. Phys. Chem. C* **2019**, *123*, 5578–5582.
- (28) Granda-Marulanda, L. P.; Builes, S.; Koper, M. T. M.; Calle-Vallejo, F. Influence of Van Der Waals Interactions on the Solvation Energies of Adsorbates at Pt-Based Electrocatalysts. *ChemPhysChem* **2019**.
- (29) Magnussen, O. M.; Groß, A. Toward an Atomic-Scale Understanding of Electrochemical Interface Structure and Dynamics. *Journal of the American Chemical Society*. American Chemical Society March 27, 2019, pp 4777–4790.
- (30) Bodenschatz, C. J.; Zhang, X.; Xie, T.; Arvay, J.; Sarupria, S.; Getman, R. B. Multiscale Sampling of a Heterogeneous Water/Metal Catalyst Interface Using Density Functional

- Theory and Force-Field Molecular Dynamics. J. Vis. Exp. 2019, 2019.
- (31) Saleheen, M.; Heyden, A. Liquid-Phase Modeling in Heterogeneous Catalysis. *ACS Catalysis*. UTC 2018, pp 2188–2194.
- (32) Saleheen, M.; Zare, M.; Faheem, M.; Heyden, A. Computational Investigation of Aqueous Phase Effects on the Dehydrogenation and Dehydroxylation of Polyols over Pt(111). *J. Phys. Chem. C* **2019**, *123*, 19052–19065.
- (33) Zhang, X.; Sewell, T. E.; Glatz, B.; Sarupria, S.; Getman, R. B. On the Water Structure at Hydrophobic Interfaces and the Roles of Water on Transition-Metal Catalyzed Reactions: A Short Review. *Catal. Today* **2017**, *285*, 57–64.
- (34) Zhang, X.; Defever, R. S.; Sarupria, S.; Getman, R. B. Free Energies of Catalytic Species Adsorbed to Pt(111) Surfaces under Liquid Solvent Calculated Using Classical and Quantum Approaches. *J. Chem. Inf. Model.* **2019**, *59*, 2190–2198.
- (35) Dasetty, S.; Meza-Morales, P. J.; Getman, R. B.; Sarupria, S. Simulations of Interfacial Processes: Recent Advances in Force Field Development. *Current Opinion in Chemical Engineering*. Elsevier Ltd March 1, 2019, pp 138–145.
- (36) Hussain, J.; Jónsson, H.; Skúlason, E. Calculations of Product Selectivity in Electrochemical CO2 Reduction. *ACS Catal.* **2018**, *8*, 5240–5249.
- (37) Hussain, J.; Jónsson, H.; Skúlason, E. Faraday Efficiency and Mechanism of Electrochemical Surface Reactions: CO2 Reduction and H2 Formation on Pt(111). *Faraday Discuss.* **2016**, *195*, 619–636.
- (38) Singh, N.; Campbell, C. T. A Simple Bond-Additivity Model Explains Large Decreases in Heats of Adsorption in Solvents Versus Gas Phase: A Case Study with Phenol on Pt(111) in Water. *ACS Catal.* **2019**, *9*, 8116–8127.
- (39) Carey, S. J.; Zhao, W.; Mao, Z.; Campbell, C. T. Energetics of Adsorbed Phenol on Ni (111) and Pt (111) by Calorimetry. *J. Phys. Chem. C* **2018**, *123*, 7627–7632.
- (40) Singh, N.; Sanyal, U.; Fulton, J. L.; Gutiérrez, O. Y.; Lercher, J. A.; Campbell, C. T. Quantifying Adsorption of Organic Molecules on Platinum in Aqueous Phase by Hydrogen Site Blocking and in Situ X-Ray Absorption Spectroscopy. *ACS Catal.* **2019**, *9*, 6869–6881.
- (41) Sander, R. Henry's Law Constants "in NIST Chemistry WebBook, NIST Standard Reference Database Number 69, Eds. *PJ Linstrom WG Mallard, Natl. Inst. Stand. Technol. Gaithersbg. MD* **2000**, *20899*.
- (42) Stuckless, J. T.; Starr, D. E.; Bald, D. J.; Campbell, C. T. Metal Adsorption Calorimetry and Adhesion Energies on Clean Single-Crystal Surfaces. *J. Chem. Phys.* **1997**, *107*, 5547–5553.
- (43) Hemmingson, S. L.; Campbell, C. T. Trends in Adhesion Energies of Metal Nanoparticles on Oxide Surfaces: Understanding Support Effects in Catalysis and Nanotechnology. *ACS Nano* **2017**, *11*, 1196–1203.
- (44) Atkins, P.; de Paula, J. *Physical Chemistry: Thermodynamics, Structure, and Change*, 10th editi.; Oxford University Press: Oxford, 2014.
- (45) Zhao, W.; Carey, S. J.; Morgan, S. E.; Campbell, C. T. Energetics of Adsorbed Formate and Formic Acid on Ni(111) by Calorimetry. *J. Catal.* **2017**, *352*, 300–304.
- (46) Karp, E. M.; Silbaugh, T. L.; Crowe, M. C.; Campbell, C. T. Energetics of Adsorbed Methanol and Methoxy on Pt(111) by Microcalorimetry. *J. Am. Chem. Soc.* **2012**, *134*, 20388–20395.
- (47) Israelachvili, J. Intermolecular and Surface Forces, 3rd ed.; Academic Press, 2011.

- (48) Badachhape, R. B.; Gharpurey, K.; Biswas, A. B. Density and Surface Tension of Phenol, (Mono-, Di-, and Tri-) Chlorophenols, Salol, and (o-and m-)Chloronitrobenzenes. *J. Chem. Eng. Data* **1965**, *10*, 143–145.
- (49) Padday, J. F.; Russell, D. R. The Measurement of the Surface Tension of Pure Liquids and Solutions. *J. Colloid Sci.* **1960**, *1*, 503–511.
- (50) Zhao, W.; Carey, S. J.; Mao, Z.; Campbell, C. T. Adsorbed Hydroxyl and Water on Ni(111): Heats of Formation by Calorimetry. *ACS Catal.* **2018**, *8*, 1485–1489.
- (51) Carey, S. J.; Zhao, W.; Campbell, C. T. Energetics of Adsorbed Benzene on Ni(111) and Pt(111) by Calorimetry. *Surf. Sci.* **2018**, *676*, 9–16.
- (52) Carey, S. J.; Zhao, W.; Harman, E.; Baumann, A. K.; Mao, Z.; Zhang, W.; Campbell, C. T. Energetics of Adsorbed Methanol and Methoxy on Ni(111): Comparisons to Pt(111). ACS Catal. 2018, 8, 10089–10095.
- (53) Lew, W.; Crowe, M. C.; Karp, E.; Campbell, C. T. Energy of Molecularly Adsorbed Water on Clean Pt(111) and Pt(111) with Coadsorbed Oxygen by Calorimetry. *J. Phys. Chem. C* **2011**, *115*, 9164–9170.
- (54) Silbaugh, T. L.; Karp, E. M.; Campbell, C. T. Energetics of Formic Acid Conversion to Adsorbed Formates on Pt(111) by Transient Calorimetry. *J. Am. Chem. Soc.* **2014**, *136*, 3964–3971.
- (55) Carey, S. J.; Zhao, W.; Campbell, C. T. Bond Energies of Adsorbed Intermediates to Metal Surfaces: Correlation with Hydrogen–Ligand and Hydrogen–Surface Bond Energies and Electronegativities. *Angew. Chemie Int. Ed.* **2018**, *57*, 16877–16881.
- (56) Ketcham, W. M.; Hobbs, P. V. An Experimental Determination of the Surface Energies of Ice. *Philos. Mag.* **1969**, *19*, 1161–1173.
- (57) Tyson, W. R.; Miller, W. A. Surface Free Energies of Solid Metals: Estimation from Liquid Surface Tension Measurements. *Surf. Sci.* **1977**, *62*, 267–276.
- (58) Vitos, L.; Ruban, A. V; Skriver, H. L.; Kollar, J. The Surface Energy of Metals. *Surf. Sci.* **1998**, *411*, 186–202.
- (59) Chibowski, E.; Perea-Carpio, R. Problems of Contact Angle and Solid Surface Free Energy Determination. *Advances in Colloid and Interface Science*. 2002, pp 245–264.
- (60) Müller, P.; Kern, R. Equilibrium Nano-Shape Changes Induced by Epitaxial Stress (Generalised Wulf-Kaishew Theorem). *Surf. Sci.* **2000**, *457*, 229–253.

Table of Contents Graphic:

